Electronic Supplementary Information

New Cu(I) square grid-type and Ni(II) triangle-type complexes: synthesis and characterization of effective binders of DNA and serum albumins

Martyna Szymańska[a], Maciej Kubicki[a], Giovanni N. Roviello[b], Giuseppe Consiglio[c], Marta A. Fik-Jaskółka[a*] and Violetta Patroniak[a]

[a]Faculty of Chemistry, Adam Mickiewicz University, Uniwersytetu Poznańskiego 8, 61-614 Poznań, Poland

[b] Institute of Biostructures and Bioimaging – CNR, Area di Ricerca site and Headquartes, Via Tommaso De Amicis, 95, 80145 Napoli, Italy

[c]Dipartimento di Scienze Chimiche, Università degli studidi Catania, viale A. Doria 6, I-95125 Catania, Italy

[*]Corresponding author
E-mail address: martafik@amu.edu.pl

Dedicated to Professor Paolo Finocchiaro on the occasion of 80th birthday.

Table S1 Relevant geometrical parameters (Å, °) with su's in parentheses. [i] denotes the symmetry operation 1-x,1-y,1-z. For ***C2*** *three larges ngles around Ni centers are listed. A and B are mean planes of the quinoline moieties in the ligand molecules.*

C1		**C2**	
Cu1-N19A	2.002(2)	Ni1-N1A	2.174(4)
Cu1-N19B[i]	2.007(2)	Ni1-N1C	2.200(4)
Cu1-N22A	2.055(2)	Ni1-N12A	2.086(4)
Cu1-N22B[i]	2.051(2)	Ni1-N12C	2.074(4)
Cu2-N1A	2.025(2)	Ni1-N1E	2.071(5)
Cu2-N1B	2.023(2)	Ni1-O1H	2.055(4)
Cu2-N12A	1.994(2)	Ni2-N19A	2.087(4)
Cu2-N12B	1.993(2)	Ni2-N19B	2.068(4)
		Ni2-N22A	2.194(4)

N19A-Cu1-N19B^{i}	135.61(10)	Ni2-N22B	2.157(4)
N19A-Cu1-N22B^{i}	124.95(9)	Ni2-N1D	2.088(5)
N22B-Cu1-N19B^{i}	81.53(10)	Ni2-O1I	2.086(5)
N19A-Cu1-N22A	81.25(9)	Ni3-N1B	2.161(5)
N19B-Cu1^{i}-N22A	119.53(9)	Ni3-N12B	2.083(4)
N22B-Cu1^{i}-N22A	118.72(9)	Ni3-N19C	2.071(4)
N12A-Cu2-N12B	124.46(9)	Ni3-N22C	2.144(4)
N1B-Cu2-N12B	81.91(10)	Ni3-N1F	2.103(5)
N12A-CU2-N1B	124.35(10)	Ni3-N1G	2.103(5)
N1A-Cu2-N12B	125.11(9)		
N1A-Cu2-N12A	80.96(9)	Ni1	174.38(17) 174.08(16) 172.01(18)
N1A-Cu2-N1B	126.32(9)	Ni2	176.43(18) 173.73(17) 172.89(16)
		Ni3	177.55(19) 173.71(16) 170.30(16)
A/B	6.56(6) 7.01(7)	A/B	46.34(15) 14.6(2) 29.19(15)

a)

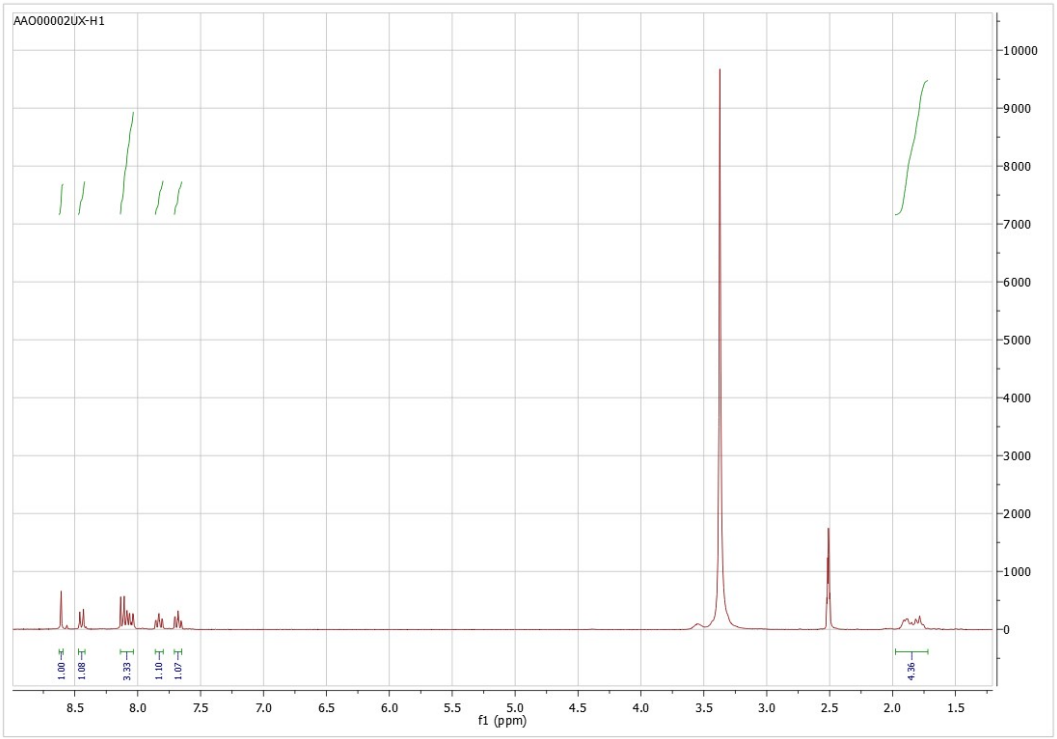

b)

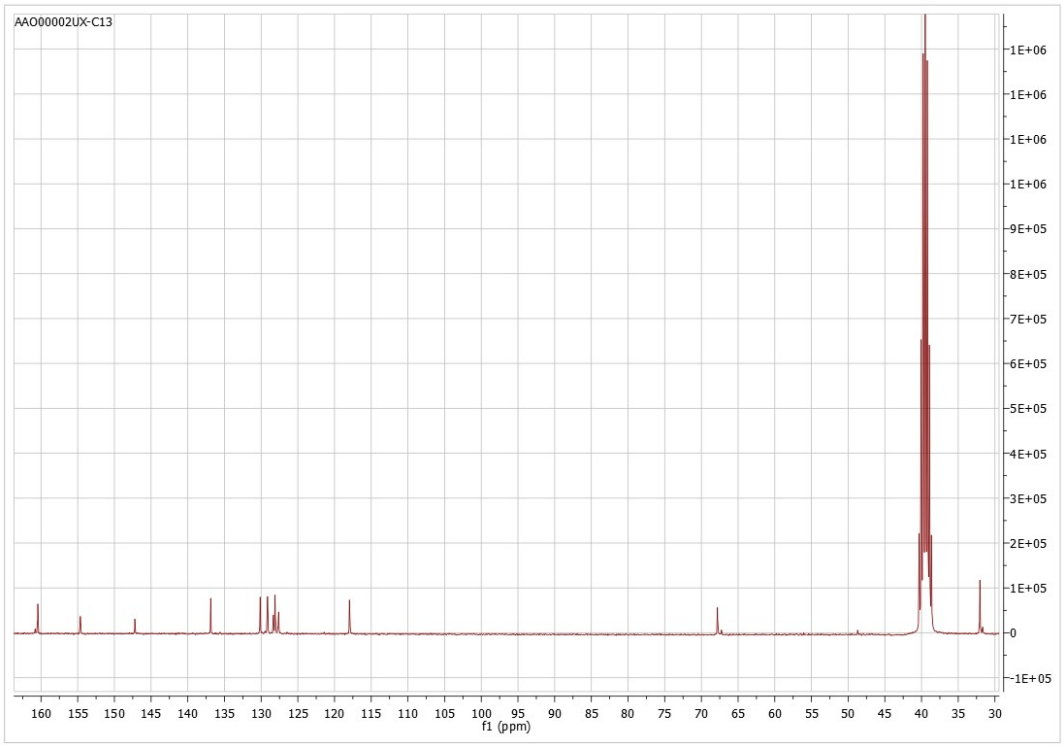

*Figure S1 (a) [1]H NMR (300 MHz, DMSO-d_6) spectrum of ligand **L**: δ (ppm) = 8.60 (s, 1H); 8.44 (d, 1H); 8,07 (m, 3H), 7.82 (t, 1H); 7.67 (t, 1H); 1.82 (dt, 4H). (b) [13]C NMR (75 MHz, DMSO-d_6) spectrum of ligand **L**: δ (ppm) = 160.47; 154.67; 147.24; 136.9; 130.16; 129.16; 128.36; 128.13; 127.65; 117.95; 67.84; 32.08 (2C).*

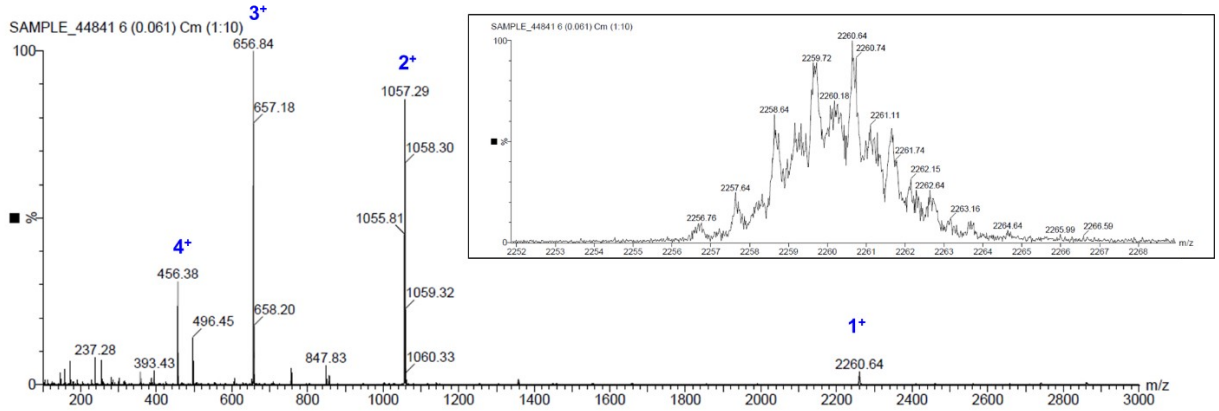

*Figure S2 ESI-MS spectrum of **C1.***

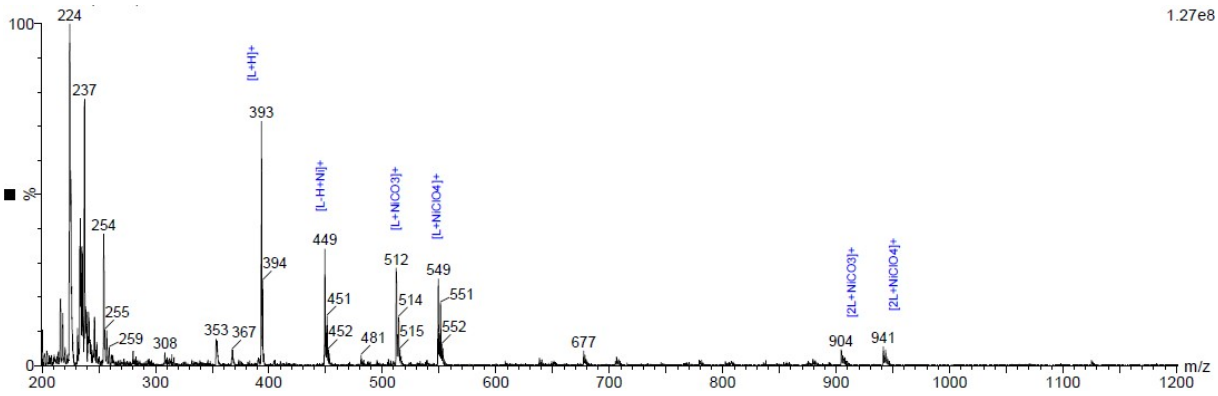

*Figure S3 ESI-MS spectrum of **C2.***

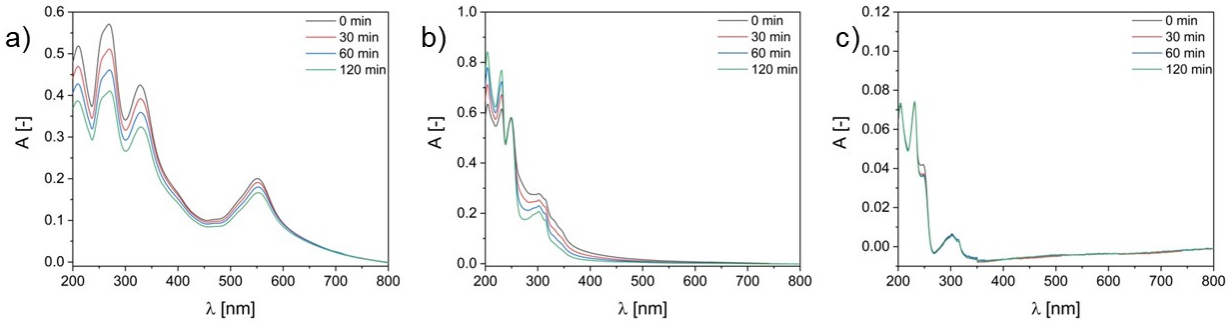

*Figure S4 Stability tests complex **C1**[a)], complex **C2** [b)] and ligand **L** [c)] in Tris-HCl (5 mM Tris, 50 mM NaCl, pH = 7.22)*

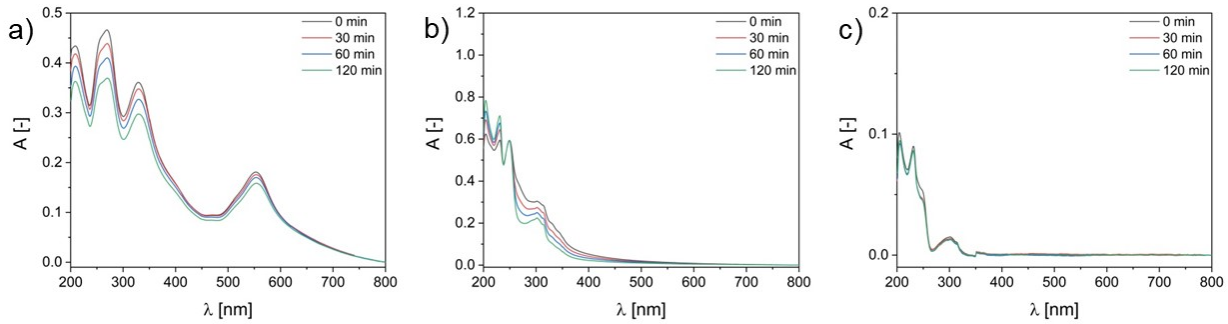

*Figure S5 Stability tests complex **C1** [a)], complex **C2** [b)] and ligand **L** [c)] in PBS buffer (0.01 M phosphate buffer, 0.0027 M potassium chloride, 0.137 M sodium chloride pH = 7.4)*

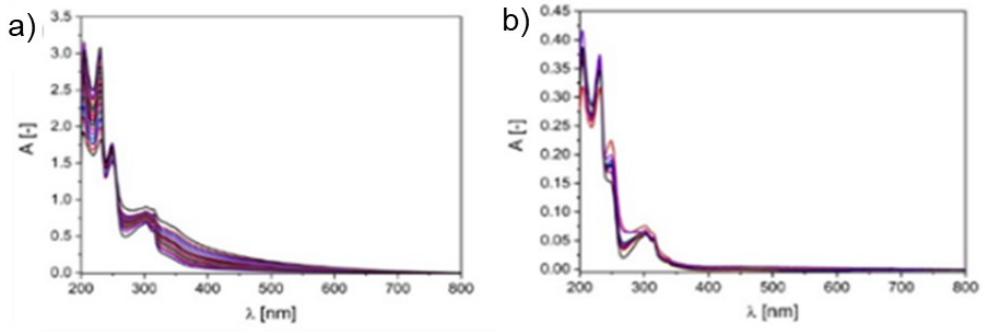

*Figure S6 Absorption titration of $[Ni_3L_3]^{6+}$ triangle **C2** (a) and **L** (b) with increasing concentrations of CT-DNA (0-100 μM) in buffer Tris-HCl (5 mM Tris, 50 mM NaCl, pH = 7.22).*

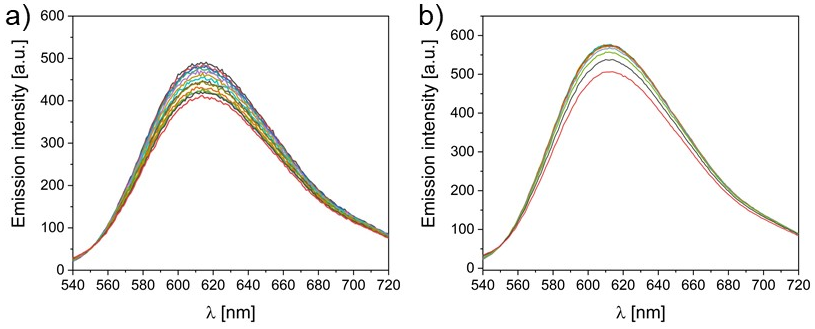

*Figure S7 Emission spectra of ethidium bromide bound to CT-DNA in the presence of increasing amounts of complex **C2** (0-100 μM, (a)) and ligand **L** (0-100 μM), (b)) in buffer Tris-HCl (5 mM Tris, 50 mM NaCl, pH = 7.22).*

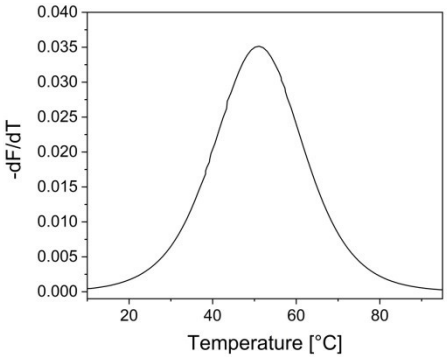

Figure S8 First derivative of the experimental melting curve of d(GTTAATCGCTGG) DNA alone (2.5 µM).

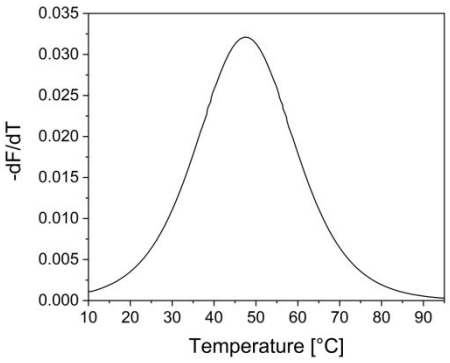

*Figure S9 First derivative of the experimental melting curve of ligand **C1** (10 µM) and d(GTTAATCGCTGG) DNA (2.5 µM).*

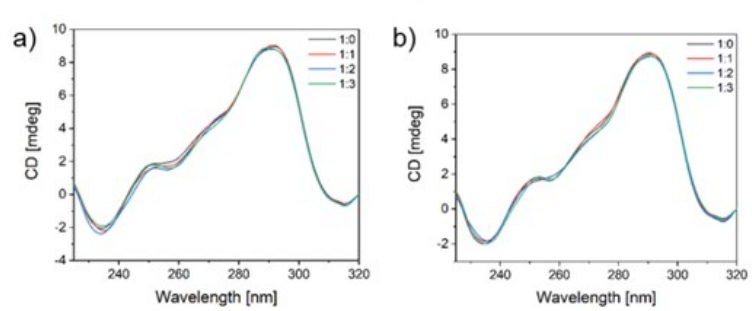

Figure S10. Tel22 folded (2 µM) in buffer Tris-HCl (10 mM Tris, 100 mM KCl) pH=7.5 in the presence of increasing concentration of grid C1 (0-6 µM, on the left) and triangle C2 (0-6 µM, on the right). The molar ratios of tel22:compound is presented on the graph. The folded Tel22 in K^+ solutions possesses characteristic spectrum - a negative band at 240 nm, the positive band at 290 nm and the shoulder between 250-260 nm [1, 2]. Upon addition of C1 and C2 the conformational changes visible in CD are only slight and seem to indicate that they do not significantly influence the secondary structure of GQ.

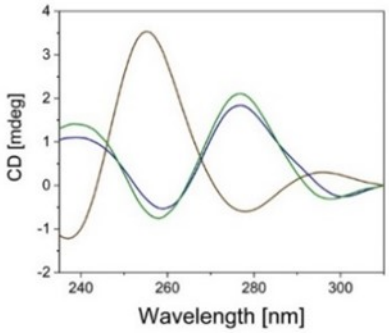

*Figure S11. ICD spectra of randomly folded Tel22 (2 μM) with the triangle **C2** (buffer with 10 mM Tris, pH=7.5). Molar ratios Tel22:compound: brown – 1:0; blue – 1:1; green line – 1:2. The assembly is characterized by a spectrum with positive peaks at ca. 240 nm and 280 nm and negative peaks at ca. 260 nm and 300 nm.*

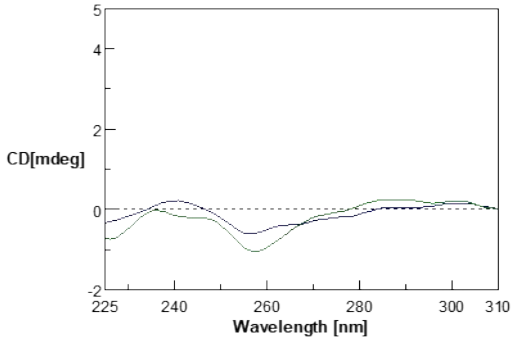

*Figure S12. ICD spectra of randomly folded Tel22 (2 μM) with the grid **C1** (buffer with 10 mM Tris, pH=7.5). Molar ratios Tel22:compound: blue line – 1:2; green line – 1:4.*

References:

1. A. Ambrus, D. Chen, J. Dai, T. Bialis, R. A. Jones and D. Yang, *Nucleic Acids Res.*, 2006, **34**, 2723-2735.
2. I. Prislan, S. Sajko, N. P. Ulrih and L. Fürst, *RSC Adv.*, 2019, **9**, 41453-41461.